



A study on thermal energy storage using open adsorption system

دراسة على تخزين الطاقة الحرارية باستخدام نظام الامتصاص المفتوح

Hesham O. Helaly, Mohamed M. Awad, Ibrahim I. El-Sharkawy and Ahmed M. Hamed

KEYWORDS:

Adsorption; Thermal energy storage; Silica gel, Heat and mass transfer; COMSOL Multi-physics.

المخلص العربي:- يعرض هذا البحث دراسة نظرية وعملية لطريقة تخزين الطاقة الحرارية باستخدام نظام امتصاص مفتوح حيث تم استخدام السيلكا جيل كمتن. يدرس النموذج النظري عمليات انتقال الكتلة والطاقة في النظام والتي تم حل معادلاتها باستخدام برنامج COMSOLTM. وتم عمل تجارب معملية لدراسة تأثير تغير معدل التدفق والرطوبة النسبية على كمية الطاقة المخزنة. النتائج تشمل درجات الحرارة الخارجة من النظام وكثافة تخزين الطاقة خلال عملية الامتزاز وتحليلها لمختلف الظروف. أظهرت النتائج أن هناك مفاضلة بين كمية الطاقة المنطلقة ودرجة الحرارة الخارجة لذا يجب اختيار الأمثل بينهم قبل اختيار معدل التدفق المناسب. كما أظهرت النتائج أن كثافة الحرارة المخزنة ودرجة الحرارة المنطلقة تزداد مع زيادة رطوبة الهواء الداخل للنظام. كانت أكبر كمية حرارة منطلقة عمليا من الجهاز 325.8 MJ/m^3 أو 90.5 kWhr/m^3 وبالنسبة لظروف التشغيل المحددة والافتراضات المذكورة، تظهر القياسات التجريبية اتفاقا مقبولا مع الحل التحليلي.

Abstract—Theoretical and experimental investigation on the thermal energy storage of an open adsorption system is presented. Laboratory experiments have been conducted, using silica gel as adsorbent, to study the effect of flow rate and inlet relative humidity on the amount of energy stored. The theoretical model, used to describe the mass and energy transfers in the system, was solved using COMSOLTM software. The model was validated against laboratory experiments performed at varying conditions. Temperature and energy density profiles during the adsorption process have been analyzed for various conditions. Results show that the storage density increases with the increase of the flow rate. However, at higher flow rates lower discharge

temperatures are obtained. So, an optimization is recommended before choosing the operating flow rate. Furthermore, results show that the higher the air inlet relative humidity, the higher the energy density and the higher the discharge temperature. The maximum energy density obtained for a bed volume of $5.09 \times 10^{-4} \text{ m}^3$ is 325.8 MJ/m^3 . For the predefined working conditions and assumptions, the numerical solution shows satisfied agreement with the experimental measurements.

I. INTRODUCTION

IN Egypt, about 45% of utilized energy is used for air-conditioning and heating processes [1]. Thermal energy storage (TES) is considered an important energy conservation technology and, recently, increasing attention has been paid to its utilization, especially for HVAC applications [2]. In TES, energy in the form of heat or cold can be placed in a storage medium for a particular duration and can be retrieved from the same location for later usage [3].

There are several ways to store thermal energy by sensible heat, by latent heat, by thermochemical or combination of these methods. In sensible heat storage, the heat energy stored in the material is directly related to specific heat capacity and

Received: 21 May, 2018 - accepted: 24 July, 2018

H. O. Helaly is Instructor at the High Institute of Engineering and technology in new Damietta, Damietta, Egypt. (e-mail: h_o_helaly@students.mans.edu.eg).

I. I. El-Sharkawy is Prof. of Mechanical Power Engineering, Faculty of Engineering, Mansoura University, Egypt. Mansoura (e-mail: ielsharkawy@mans.edu.eg).

A. M. Hamed is Prof. of Mechanical Power Engineering, Faculty of Engineering, Mansoura University, Egypt. Mansoura (e-mail: amhamed@mans.edu.eg).

M. M. Awad is Ass. Prof. of Mechanical Power Engineering, Faculty of Engineering, Mansoura University, Egypt. Mansoura (e-mail: m_m_awad@mans.edu.eg).

temperature difference of the material. Water, rock and soil are the most common materials in sensible energy storage applications [4]. In latent heat storage, the heat storage material undergoes a phase transformation process for storing or discharging the heat energy. The materials used to store latent heat are known as Phase Change Materials (PCMs). These storage substances are generally ice, paraffin, salts, fatty acids and other mixtures [5]. In thermochemical heat storage, energy is stored after a dissociation reaction and afterward recovered in a reverse chemical reaction. This chemical heat energy can be stored and reused throughout a long-term storage application [6].

The selection of a TES is mainly dependent on the storage period required (i.e., diurnal, weekly or seasonal), economic viability, operating conditions, etc [7]. For the types of TES, sensible and latent TES were already developed for many years for commercial applications [8]. In recent years, thermochemical thermal energy storage systems are increasingly fast as they become promising options for thermal heat storage [9]. In comparison to conventional heat storages, they offer some advantages. Their energy density is comparatively high, e.g. about 2–3 times higher than in conventional heat storage mediums. They also can store thermal energy for longer periods with limited heat loss as it can be stored at near ambient temperature [10].

Thermochemical storage can be divided into chemical reaction and sorption [11]. “Sorption” is a general term which encompasses both absorption and adsorption. Adsorption means the binding of a gaseous or liquid phase of a component on the inner surface of a porous material [12]. In adsorption process, thermal energy can be stored through three steps:

Charging (Regeneration step): Heat is put into the adsorbent to remove the adsorbate. This heat source can be provided by either waste heat sources or solar energy to avoid the reducing of natural resources and environmental pollution.

Storing: TES can be achieved by sealing the material from the surroundings. After desorption, the adsorbent and the adsorbent can theoretically remain in the charged state without any thermal losses due to the storage period until the adsorption process is activated.

Discharging: (Adsorption), Adsorption is an exothermic physical process where a gas diffuses into the pores of a porous solid material and is trapped into the crystal lattice which releases heat [13].

The utilization of the adsorption-desorption cycle as a means of thermal energy storage was first proposed by Close and Pryor [14]. In Munich, Hauer [15, 16] reported a successful open adsorption system using 7000 kg zeolite 13X, which was installed in a school and connected to the local district heating network to offset the peak energy demands, performing at a storage density of 446 MJ/m³. Gantenbein et al. [17] have investigated a storage system with both silica gel and zeolite as adsorbents. An energy density of 381 MJ/m³ was achieved. Dawoud *et al.* [18] performed experiments using zeolite 13X and water and obtained an energy density of 518 MJ/m³. In the “SolSpaces” project [19], special attention was given to the large heat capacities issue. The main idea is

to divide the sorption store into several sectors, which can be adsorbed or desorbed separately. It is expected that over 90 % of the heat demand for room heating and over 80 % of the heat demand for residential hot water preparation can be covered by the solar thermal system combined with the sorption store. Hauer and Fischer [20] used zeolite 13X into a dishwasher to decrease the energy consumption by means of an open adsorption system. The reduction of the energy consumption compared to a traditional dishwasher from about 1.05 kWh to 0.80 kWh per washing cycle leads to energy savings of about 24 %. To increase the storage density, Dicaire and Tezel [21, 22] tested different adsorbents at varying flow rates and different values of relative humidity to determine the optimal operating conditions. A maximum energy density of 576 MJ/m³ has been achieved with the AA/13X as adsorbent.

Although sorption thermal storage systems have some advantages, they seem to have more complexity than other storing methods such as; expensive investment, poor heat and mass transfer ability and low heat storage density in actual systems. To overcome these barriers, extensive academic efforts are now being carried out worldwide [23].

Accordingly, a silica gel–water adsorptive heat storage is experimentally investigated throughout this work. It is aimed to simulate the discharge temperature of the thermal energy storage unit and predict the amount of energy stored in it. This simulation is accomplished through developing a mathematical model using COMSOL Multi-physics software [24] to solve it. The simulated results will be validated against experimental results for various operating conditions.

II. EXPERIMENTAL STUDY

The experiments were conducted at various flowrates and relative humidities to optimize the operating conditions and to validate the results with the mathematical model. Water was identified as an adsorbate and Silica gel as an adsorbent. Fig 1 provides a detailed flow diagram of the various components in the system.

A. Experimental Set-Up

Fig 2 shows a view of the thermal energy storage unit. It is composed of the adsorption packed bed, two centrifugal blowers, evaporative bed, electric heater and four ball valves. The packed bed is stainless steel cylinder with a volume of $5.09 \times 10^{-4} m^3$ and its inner diameter is 101.6 mm. The bed inlet and outlet are blocked with a narrow stainless-steel net. The bed is insulated using glass wool. The air comes from two air blowers and goes through the wet and dry cylinders. The 1200-W electric heater is used to control the inlet temperature during adsorption and regeneration processes.

B. Instrumentation

Test 435 indoor air quality meter is used to measure the inlet temperature and relative humidity of air in addition the inlet air velocity using different probes. The accuracy of the temperature probe is $\pm 0.2^\circ C$ and that of relative humidity

is 0.1 %RH. The accuracy of the velocity is 0.01 m/s. accuracy of $\pm 0.2^{\circ}\text{C}$.
 Temperatures have been measured using K-type thermocouples at different positions in the bed with an

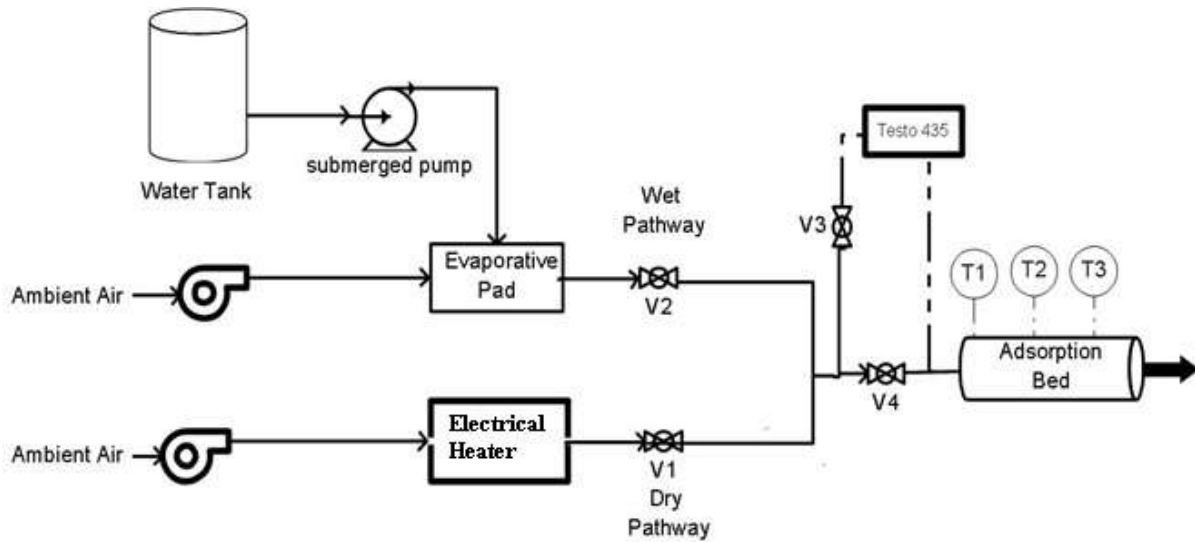


Fig 1 Schematic diagram of experimental set-up

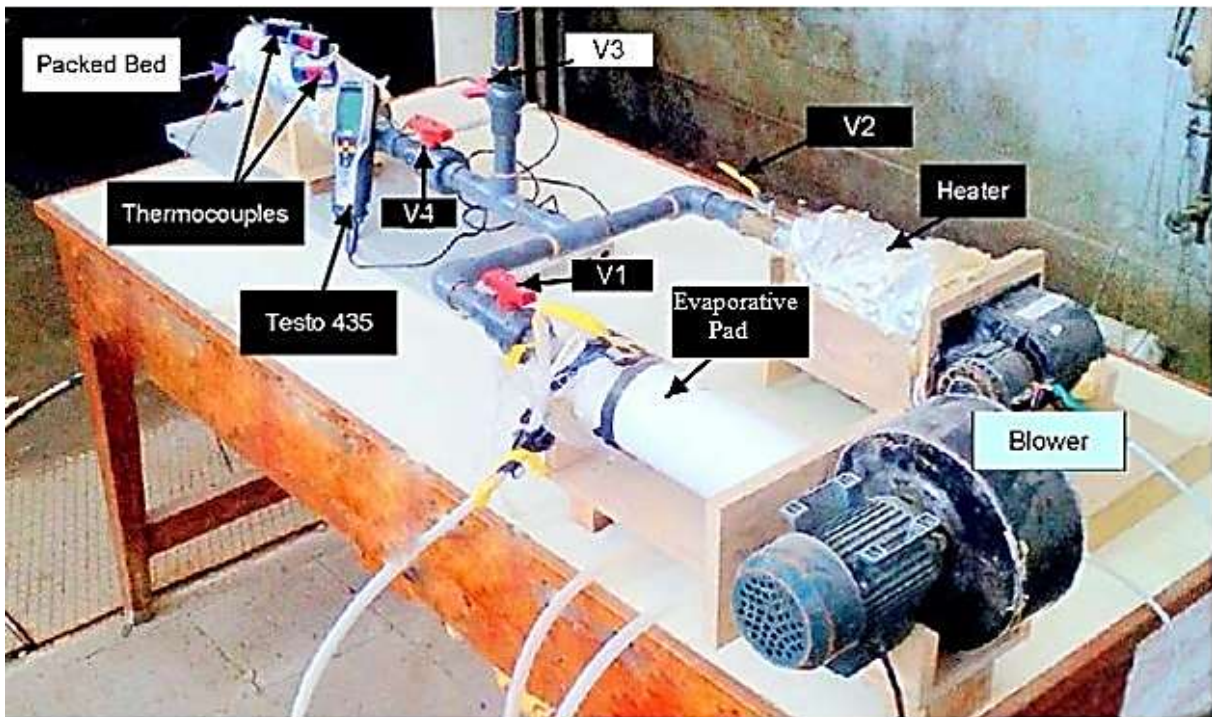


Fig 2 Pictorial view of the system

C. Experimental Procedure

Experimental procedure is composed of three steps: regeneration, storing and adsorption.

1. During the regeneration process (charging) a hot air is passed through the bed to remove the adsorbate. Inlet airflow is heated using the electric heater. Hot dry air at

120°C with humidity ratio of 10 g/kg is allowed to pass through the bed for two hours.

2. The storing process is conducted by sealing the column directly after the regeneration process and the column was allowed to cool to room temperature.

3. The adsorption process (discharging) is done by introducing air with high relative humidity through the bed. Adsorption process has been conducted according to the following steps:
 - a. Before turning on the centrifugal blowers, valve (4) is set totally closed and valves (1, 2, and 3) are set totally open.
 - b. The submerged pump is started to circulate water over the evaporative pads.
 - c. The two centrifugal blowers are turned on. The evaporative pad path produces air with high relative humidity (RH) whereas the other path air produces air with low RH.
 - d. By combining different flows from the two paths, the desired relative humidity and flow rate can be reached.
 - e. After the relative humidity and flow rate are set, valve (3) is closed and valve (4) is set totally open and the humid air passes through the bed.

III. THEORETICAL MODEL

The model, which describes an open flow system, is schematically presented in Fig 3. During adsorption, moist air with a specified inlet moisture concentration $c_{(g,in)}$ and temperature T_{in} flows with a velocity v_g through a porous cylinder (adsorbent) of initial moisture content q_{in} , length L and inlet radius r_c . The moisture concentration in the adsorbent q . Assumptions made before modeling the process are mentioned below:

1. The airflow passing through the bed is one-dimensional and steady.
2. The transport processes within the adsorbent bed are transient convection and diffusion of heat and water vapor.
3. The properties of the adsorbent particles are homogeneous.
4. The linear driving force (LDF) model is used to predict the sorption rate by considering both the solid side and the gas side mass transfer resistances.
5. Instantaneous adsorption on the pellet surface [21].

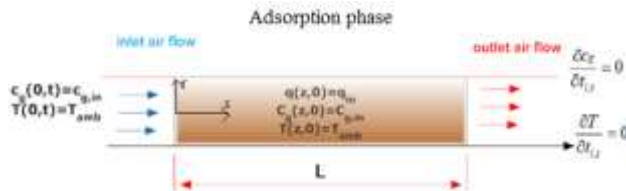


Fig 3 Theoretical model schematic

A. Solid side mass balance

Adsorption uptake is approximately given by the linear driving force (LDF), which was first proposed by Gleuckauf and Coates [25], expressed by the difference of the amount adsorbed, q , and the amount adsorbed in equilibrium q_e .

$$\frac{dq}{dt} = K(q_e - q) \quad (1)$$

where K is the overall mass transfer coefficient and is

calculated using Eq. 2.

$$K = \frac{15 D_{so} \exp\left(-\frac{E_a}{RT}\right)}{r_p^2} \quad (2)$$

where r_p is the adsorbent particle radius, and R the universal gas constant. D_{so} is the pre-exponential constant, which has a value of $2.54 \times 10^{-4} m^2/s$ and E_a is the activation energy which has a value of $4480 J/mol$ characteristics [26].

The initial condition for the water mass balance in the pellet is given by Eq. 1, which is calculated using Temperature-Dependent Toth isotherm at the regeneration conditions.

$$q|_{t=0} = q_{in} \quad (\text{for all } z \text{ and } r \text{ values}) \quad (3)$$

B. Gas side mass balance

The mass balance in the bulk phase of the column is described by Geankoplis [27] as follows,

$$\epsilon_c \frac{\partial c_g}{\partial t} = \epsilon_c D_z \frac{\partial^2 c_g}{\partial z^2} - \epsilon_c v_g \frac{\partial c_g}{\partial z} - \rho_p \frac{\partial q}{\partial t} \quad (4)$$

The terms in Eq. 4 represent the material accumulation, the axial diffusion due to the concentration gradient, the convection due to flow, and the mass transfer due to adsorption respectively.

The parameters in Eq. 4 include the column void fraction (ϵ_c), the bulk gas concentration in the column (c_g), the axial dispersion coefficient (D_z), the superficial gas velocity (v_g), the pellet density (ρ_p), and the rate of water adsorption $\frac{\partial q}{\partial t}$. The corresponding initial and boundary conditions for the material balance in the bulk phase of the column include:

$$c_g|_{t=0} = c_{g,inlet} \quad (\text{for all } z \text{ and } r \text{ values}) \quad (5)$$

$$c_g|_{z=0} = c_{g,inlet} \quad (\text{for all } z \text{ and } r \text{ values}) \quad (6)$$

$$\frac{\partial c_g}{\partial z} \Big|_{z=L} = 0 \quad (\text{for all } z \text{ and } r \text{ values}) \quad (7)$$

C. Energy balance in the column

The temperature of the gas stream (bulk phase in the column) is calculated by doing an energy balance around the column. Energy balance is done by considering the energy accumulation, conduction and convection in the column [28]. The energy balance in the column is represented using Eq.8.

$$(\rho C_p)_{eff} \frac{\partial T_g}{\partial t} + \rho_g C_{p,g} v_g \cdot \nabla T_g = \quad (8)$$

$$\nabla \cdot (k_{eff} \nabla T_g) - \frac{2h_{fd}}{r_c} (T_g - T_w) + \rho_p \Delta H_{ads} \frac{\partial q}{\partial t}$$

The parameters in Eq.7 include the effective volumetric

heat capacity at constant pressure $(\rho C_p)_{eff}$ the density of the gas stream ρ_g , the heat capacity of the gas stream $(C_{p,g})$ the superficial gas velocity (v_g) , the effective thermal conductivity (k_{eff}) , the heat transfer coefficient in the bulk phase (h_{fd}) , the column radius (r_c) , the column wall temperature (T_w) , and the heat of adsorption (ΔH_{ads}) .

The effective volumetric heat capacity of the solid-fluid system $(\rho C_p)_{eff}$ and the effective thermal conductivity of the solid-fluid system, k_{eff} are given by:

$$(\rho C_p)_{eff} = (1 - \epsilon_c)\rho_p C_{p,p} + \epsilon_c \rho_g C_{p,g} \quad (9)$$

$$k_{eff} = (1 - \epsilon_c)k_p + \epsilon_c k_g \quad (10)$$

Here the subscripts p and g refer to the porous matrix and gas phases, respectively, ρ is the density, C_p is the specific heat at constant pressure and k is the thermal conductivity, respectively. The corresponding initial and boundary conditions for the energy balance in the column include:

$$T_g|_{t=0} = T_{in} \quad (11)$$

$$T_g|_{z=0} = T_{in} \quad (12)$$

$$\frac{\partial T_g}{\partial z}|_{z=1} = 0 \quad (13)$$

D. Additional Equation

The equilibrium water concentration was calculated using the Temperature-Dependent Toth isotherm [29].

$$q_e = \frac{a P_{H_2O}}{[1 + (b P_{H_2O})^n]^{1/n}} \quad (14)$$

$$a = a_o \exp(E/T_g) \quad (15)$$

$$b = b_o \exp(E/T_g) \quad (16)$$

$$n = n_o + c/T_g \quad (17)$$

Eqs. 13-16 include the partial pressure of water (P_{H_2O}) , the gas temperature (T) , as well as the fitted Toth parameters (a_o, b_o, E, n_o, c) . The fitted parameters were obtained from experimental data from Wang and LeVan [29] and are presented in TABLE 1.

TABLE 1
TEMPERATURE-DEPENDENT TOOTH ISOTHERM PARAMETERS FOR WATER VAPOR ADSORPTION ON DIFFERENT ADSORBENTS [29]

Parameter	Silica gel
a_o (mol/kg Pa)	0.1767
b_o (1/Pa)	2.787×10^{-8}
n_o (-)	-0.00119
c (K)	22.13
E (K)	1093

Axial dispersion coefficient (D_z) is calculated based on Reynolds and Schmidt numbers which are calculated using physical properties of the gas stream [30-32] by using the following equations.

$$Re_p = \frac{\rho_g v_g D_p}{\mu_g} \quad (18)$$

$$Sc = \frac{\mu_g}{\rho_g D_m} \quad (19)$$

$$D_z = \frac{D_m}{\epsilon_c} (20 + 0.5(Re_p)(Sc)) \quad (20)$$

Packed beds cause high-pressure drop as a result of high turbulence of fluid flow through it. The pressure drop increases the blower power used to overcome the friction through the bed. The Ergun Equation [33], can be used to calculate pressure drop through the bed.

$$\frac{\Delta p}{L} = 150 \frac{\mu_g v_g}{D_p^2} \frac{(1 - \epsilon_c)^2}{\epsilon_c^3} + 1.75 \frac{\rho_g v_g^2}{D_p} \frac{(1 - \epsilon_c)}{\epsilon_c^3} \quad (21)$$

where, Δp is the pressure drop, L is the length of the packed bed, v_g is the superficial velocity, ρ_g is the fluid density, μ_g the fluid viscosity, D_p the effective particle diameter and ϵ_c the void fraction.

IV. MATHEMATICAL PROCEDURE

The modeling for the current adsorption study was performed using the COMSOL Multi-physics [24] software. "Transport of Diluted Species in Porous Media" interface is used to solve gas side mass, "Heat transfer in porous media" to solve overall energy balance and "Classical PDEs convection diffusion Equation" to solve solid side mass balance. Moreover, properties of moist air as a function of temperature and relative humidity from COMSOL model library have been used. The main data inputs are summarized in Table 2

TABLE 2
DATA INPUTS FOR THE MATHEMATICAL MODEL

Interface input	Value
Properties of Silica gel	
Bulk density (ρ_p)	750 (kg/m^3)
Porosity (ϵ_c)	0.36 (-)
Specific heat capacity (C_{pp})	1130 ($J/(kg.K)$)
Average particle radius (r_p)	0.6×10^{-3} (m)
Thermal conductivity (K_p)	0.173 ($W/(m.K)$)
Specific surface area (S_p)	5.3×10^5 (m^2/kg)
The pre-exponential constant (D_{s0})	2.54×10^{-4} (m^2/s)
The activation energy (E_a)	4480 (J/mol)
Operating conditions	
Flow rate (Q)	17, 19, 23, 28 m^3/hr
Relative humidity (ϕ)	70, 75, 80 %
Ambient temperature (T_{in})	25°C
Regeneration temperature	120 °C
Flow rate (Q)	17, 19, 23, 28 m^3/hr
Variables and equations	
Eqs. 14-21 are set as variables in the model. As they depend on the results of the model	
Transport of diluted species in porous media	
u_x	$Q/0.25 \pi D_f^2$
Diffusion	D_z
Temperature	From heat transfer interface
Heat transfer in porous media	
Fluid type	Moist air
Concentration	From Transport of Diluted Species
Reaction rate	$K(q_e - q) \times \Delta h_{ads} \times \rho_p$
Convection-Diffusion equation	
Initial value q_{in}	Based on Toth isotherms parameters at "regeneration"
equilibrium value q_e	Based on Toth isotherms parameters at "adsorption"
Reaction rate f	$K(q_e - q)$

V. RESULTS AND DISCUSSION

In the following, multiple tests were performed to understand how the operating conditions affect the energy released from the bed. The results from the experimental data are compared with the results from the theoretical model.

A. Effect of inlet flow rate

The effect of flow rate on the Silica gel packed bed was examined by varying the flow rate from 17 to 28 m^3/hr while the temperature and the inlet relative humidity were held constant at 25°C and 80 %, respectively.

The temperature values along the bed with respect to time are obtained at different positions. These values are compared with the experimental results as shown in Fig 4, 5, 6 and 7. Theoretical and experimental results show that the maximum temperatures of bed surface occur at bed exit ($x/L=1$). On the other hand, the temperature profile demonstrates a sudden

increase in temperature during the first few minutes, then a gradual decrease in temperature with time.

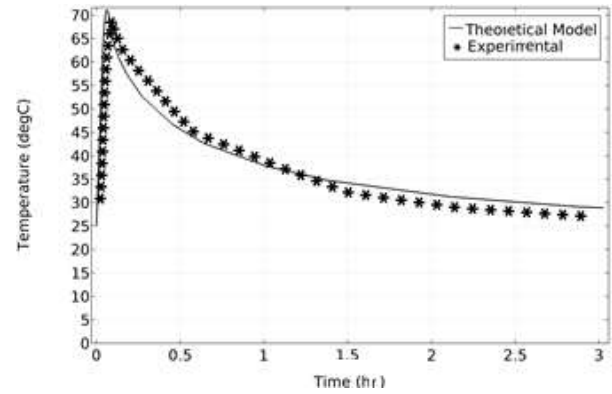


Fig 4 Variation of discharge temperature with time ($Q = 17 m^3/hr$)

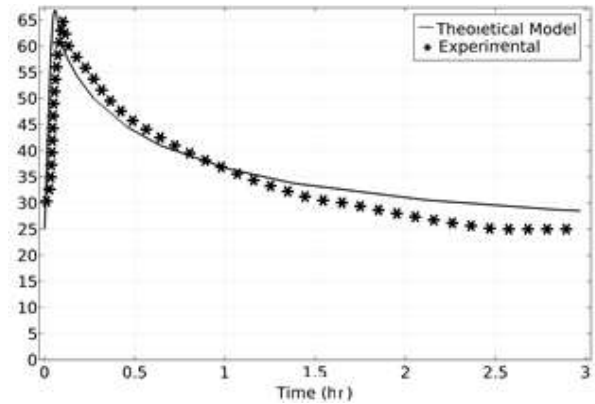


Fig 5 Variation of discharge temperature with time ($Q = 19 m^3/hr$)

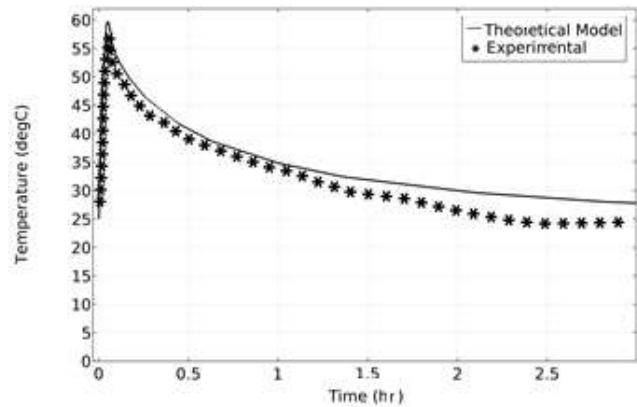


Fig 6 Variation of discharge temperature with time ($Q = 23 m^3/hr$)

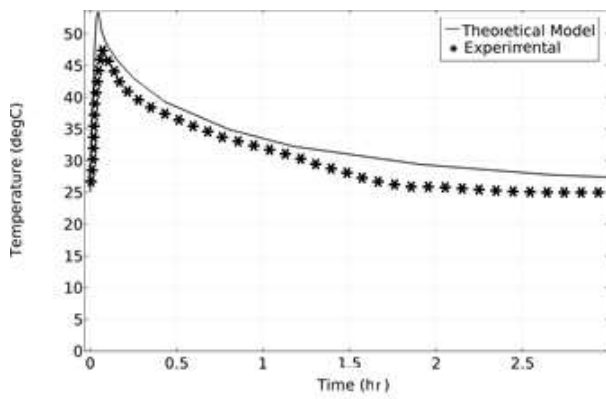


Fig 7 Variation of discharge temperature with time ($Q = 28 \text{ m}^3/\text{hr}$)

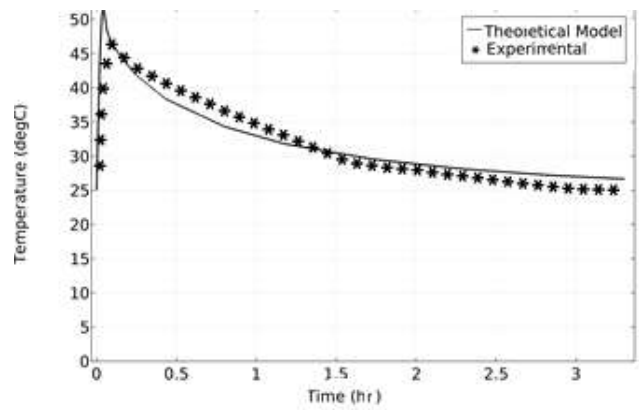


Fig 10 Variation of discharge temperature with time ($\phi = 80\%$)

B. Effect of inlet relative humidity

The inlet relative humidity was varied to investigate its effect on the system performance. Relative humidity ranging from 70% to 80% were used during the tests. The temperature values along the bed with respect to time at different positions are compared with the experimental results, for varied values of relative humidity, and shown in Fig 8, 9 and 10.

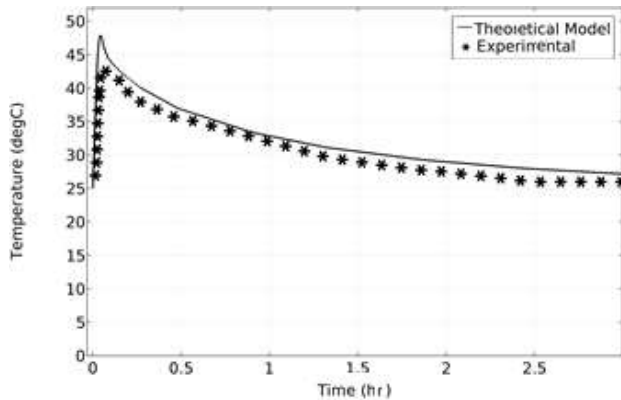


Fig 8 Variation of discharge temperature with time ($\phi = 70\%$)

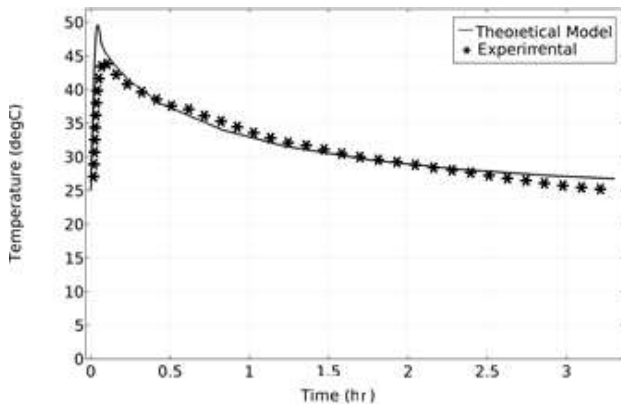


Fig 9 Variation of discharge temperature with time ($\phi = 75\%$)

C. System Energy Density

The system performance can be calculated based on the energy storage density. The amount of energy density is calculated using the following equation:

$$\text{Energy Density} = \frac{\text{Total energy released}}{\text{Column volume}} \quad (22)$$

where the total energy released is given by $\dot{m} \times C_{p,a}(T_{out} - T_{in}) \times (t_n - t_{n-1})$. $(t_n - t_{n-1})$ represents the time step between the recorded values of temperature. The packed bed with adsorbent has a volume of $5.09 \times 10^{-4} \text{ m}^3$. The energy density released from the packed bed as a function of the flow rate is shown in Fig 11. Flow rate affects the amount of released energy from the packed bed. As the flow rate decreases, the released energy decreases. That is due to the increasing of dissipated energy to the surroundings. As decreasing the flow-rate will increase the bed temperature, as shown in Fig 12.

So, an optimization, between the amount of energy needed to be stored and the temperature lift, needed to be done before choosing the operated flow rate.

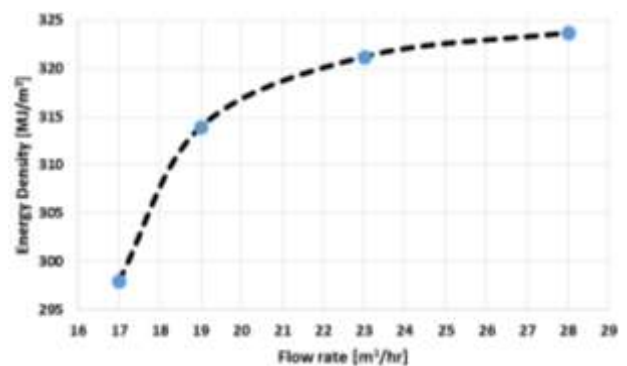


Fig 11 Energy density as a function of inlet flow rate

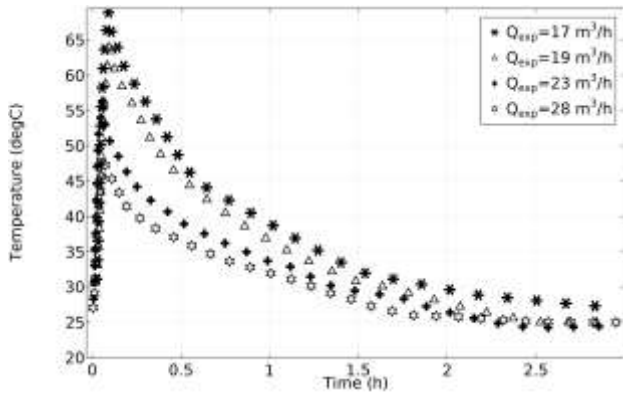


Fig 12 Outlet temperature as a function of time for varying flowrates

The inlet relative humidity of the column was varied to observe its effect on the thermal energy storage system. As the amount of water that will diffuse to reach equilibrium depends on the amount available in the vapour phase, so the value of the capacity of the adsorbent at equilibrium "q_e" will increase with the increase of the relative humidity. Therefore, as the relative humidity increases, the driving force increases, and the released energy increases. Results show that the energy released increases as the relative humidity increases. The amount of energy density and the discharge temperature as a function of inlet relative humidity are shown in Fig 13 and 14.

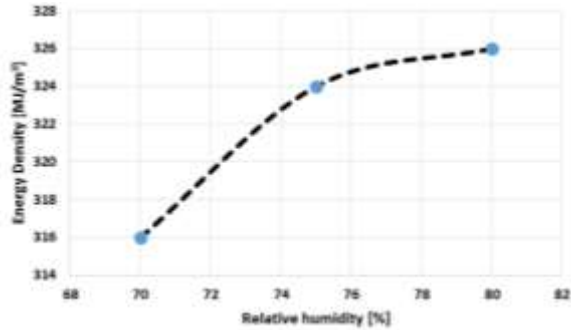


Fig 13 Energy density as a function of inlet relative humidity

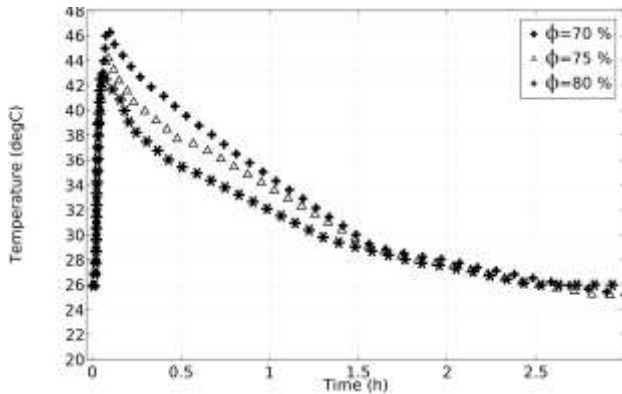


Fig 14 Discharge temperature as a function of time for varying relative humidities

VI. ERROR ANALYSIS

After modeling water vapor adsorption process in the COMSOL software, the obtained results are compared with the experimental results to estimate the accuracy of the model. This accuracy calculation is done for the outlet bed temperature by using "Mean sum of the percent errors" method, as shown below.

Mean sum of errors

$$= \frac{100}{n} \sum_{i=1}^n \left| \frac{\text{modeled data} - \text{Experiment data}}{\text{Experiment data}} \right|_i \quad (23)$$

The model estimates the bed outlet temperature with 4.66 %, 5.74 %, 5.41% and 5.53 % mean error, when compared to the laboratory experiments at flow rates 17, 19, 23 and 28 m³/h, respectively.

Furthermore, the model estimates the outlet column temperature with 5.84 %, 5.78 % and 5.32 % mean error, when compared to experiments, at inlet relative humidity 70%, 75% and 80 %, respectively.

A. Uncertainty Analysis

In this study, the measured experimental parameters are bed temperatures, flow rate, relative humidity and released energy density. Testo 435 indoor air quality meter is used to measure the inlet temperature and relative humidity of air in addition the inlet air velocity using different probes. The device has been calibrated in accredited Testo laboratories. The accuracy of the temperature probe is ± 0.2°C. The accuracy of the relative humidity probe is 0.1 %RH. The accuracy of the velocity probe is 0.01 m/s. Three thermocouples are used to measure the silica gel temperature at different positions in the bed. Temperatures have been measured using K-type thermocouples with an accuracy of ± 0.2°C.

The maximum uncertainties of the evaluated parameters are estimated by using the following expression;

$$\omega_x = \sqrt{\left(\frac{\partial X}{\partial X_1}\right)^2 \omega_{X_1}^2 + \dots + \left(\frac{\partial X}{\partial X_n}\right)^2 \omega_{X_n}^2} \quad (24)$$

Where ω_x is the uncertainty of the variable X, ω_{X_n} is the uncertainty of parameter and X_n is the parameter of interest. Analysis of experimental error shows that the maximum uncertainties in the energy density is 10.4%.

VII. CONCLUSIONS

Thermal energy storage using an open adsorption system has been theoretically and experimentally investigated. The main remarkable points of the present study can be

summarized as follows.

- 1) A detailed CFD model of heat and mass transfer in a packed bed has been presented using COMSOL software.
- 2) The model was validated against laboratory experiments with various operating conditions, which used silica gel as adsorbent.
- 3) The flow rate was varied, and we point out that an optimization, between the amount of energy needed to be stored and the temperature lift, needed to be done before choosing the operated flow rate.
- 4) Results shows that, the higher the relative humidity, the higher the discharge temperature and the energy released from the column
- 5) A maximum storage density of 325.8 MJ/m³ have been achieved at a flow rate of 30 m³/hr and a relative humidity of 80%.

VIII. NOMENCLATURE

a	Calculated Toth parameter (mol/kg/kPa)
a_0	Fitted Toth parameter (mol/kg/kPa)
b	Fitted Toth parameter (1/kPa)
b_0	Fitted Toth parameter (1/kPa)
c	Fitted Toth parameter (K)
C_g	Water concentration in the gas phase (mol/m ³)
C_{pg}	Heat capacity of the gas stream (J/kg/K)
C_{pp}	Heat capacity of the pellet (J/kg/K)
D_i	Inside diameter of the column (m)
D_m	Molecular diffusivity (m ² /s)
D_p	Diameter of the pellet (m)
D_{s0}	Pre-exponential constant (m ² /s)
D_z	Axial dispersion (m ² /s)
E	Fitted Toth parameter (K)
E_a	Activation energy (J/mol)
ΔH_{ads}	Heat of adsorption (J/mol)
h_{fd}	Heat transfer coefficient in the bulk phase (W/m ² /K)
K	Overall mass transfer coefficient (1/s)
K_a	Permeability (m ²)
K_{eff}	Effective thermal conductivity of the solid-fluid system (W/m/K)
K_g	Thermal conductivity of the gas stream (W/m/K)
K_p	Thermal conductivity of the adsorbent matrix (W/m/K)
L	Column length (m)
M_a	Molar mass of air (kg/mol)
M_w	Molar mass of water (kg/mol)
n_o	Fitted Toth parameter (-)
Δp	Pressure drop (Pa)
P_{H_2O}	Water vapor partial pressure (Pa)
P_{pa}	Column pressure (Pa)
q	Adsorbed water in the pellet ($\frac{mol_{H_2O}}{kg_{pellet}}$)
q_e	Adsorbed amount in equilibrium pellet ($\frac{mol_{H_2O}}{kg_{pellet}}$)
Re_p	Reynolds number of the particles (-)
Sc	Schmidt number (-)
S_v	Specific surface area (m ² /kg)
r_c	Inside radius of the column (m)
r_p	Pellet radius (m)
$RH\%$	Relative Humidity (%)
t	Time (s)
T	Average temperature (K)

T_g	Temperature of the gas stream (K)
T_{in}	Inlet gas stream temperature (K)
T_o	Ambient air temperature (K)
T_w	Temperature of the wall (k)
V_g	Superficial velocity of the fluid (m/s)
Greek symbols	
ϵ_c	Void fraction of the column ($\frac{m^3_{void}}{m^3_{column}}$)
μ_g	Gas stream viscosity (kg/m/s)
ρ_g	Density of the gas stream (kg/m ³)
ρ_p	Bulk density of the pellet (kg/m ³)
$(\rho C_p)_{eff}$	The effective volumetric heat capacity at constant pressure (J/m ³ /K)

REFERENCES

- [1] Egyptian Electricity Holding Company: Annual Report 2016/2017. Arab Republic of Egypt: Ministry of Electricity & Energy., 2017.
- [2] Dincer, I., On thermal energy storage systems and applications in buildings. *Energy and Buildings*, 2002. 34(4): p. 377-388.
- [3] Kalaiselvam, S. and R. Parameshwaran, *Thermal Energy Storage Technologies for Sustainability: Systems Design, Assessment and Applications* 2014: Elsevier.
- [4] Sharma, C.S., P. Harriott, and R. Hughes, An International Journal of Research and Development Thermal conductivity of catalyst pellets and other porous particles. *The Chemical Engineering Journal*, 1975. 10(1): p. 73-80.
- [5] Davis, O.C.M., *Trans. Chem. Soc.*, 1907. xci(null): p. 1666.
- [6] Sharma, A., V. Tyagi, C. Chen, and D. Buddhi, Review on thermal energy storage with phase change materials and applications. *Renewable and Sustainable Energy Reviews*, 2009. 13(2): p. 318-345.
- [7] [Kato, Y., *Thermal Energy Storage for Sustainable Energy Consumption. Chemical Energy Conversion Technologies for Efficient Energy Use*, 2007: p. 377-391.
- [8] Zalba, B., J.M. Marín, L.F. Cabeza, and H. Mehling, Review on thermal energy storage with phase change: materials, heat transfer analysis and applications. *Applied Thermal Engineering*, 2003. 23(3): p. 251-283.
- [9] Wentworth, W.E. and E. Chen, Simple thermal decomposition reactions for storage of solar thermal energy. *Solar Energy*, 1976. 18(3): p. 205-214.
- [10] Paksoy, H.Ö., *Thermal energy storage for sustainable energy consumption: fundamentals, case studies and design. Vol. 234. 2007: Springer Science & Business Media.*
- [11] Hadorn, J., Advanced storage concepts for active solar energy—IEA SHC Task 32 2003-2007. proceeding of Eurosun, Lisbon, Portugal, 2008.
- [12] Hauer, A., *SORPTION THEORY FOR THERMAL ENERGY STORAGE*, in *Thermal Energy Storage for Sustainable Energy Consumption: Fundamentals, Case Studies and Design*, H.Ö. Paksoy, Editor 2007, Springer Netherlands: Dordrecht. p. 393-408.
- [13] Ülkü, A. and M. Mobedi, Adsorption in energy storage, in *Energy Storage Systems 1989*, Springer. p. 487-507.
- [14] Close, D.J. and R.V. Dunkle, use of adsorbent beds for energy storage in drying of heating systems. *Solar Energy*, 1977. 19(3): p. 233-238.
- [15] Hauer, A. Thermal energy storage with zeolite for heating and cooling applications. in *Proceedings of 3rd Workshop of Annex. 2002.*
- [16] Hauer, A., Adsorption systems for TES—design and demonstration projects, in *Thermal Energy Storage for Sustainable Energy Consumption: Fundamentals, Case Studies and Design*, H.Ö. Paksoy, Editor 2007, Springer Netherlands: Dordrecht. p. 409-427.
- [17] Gantenbein, P., S. Brunold, F. Flückiger, and U. Frei, Sorption materials for application in solar heat energy storage. Rapperswil, Switzerland: University of applied science, 2001.
- [18] Dawoud, B., E.H. Amer, and D.M. Gross, Experimental investigation of an adsorptive thermal energy storage. *International Journal of Energy Research*, 2007. 31(2): p. 135-147.
- [19] Bertsch, F., H. Kerskes, H. Drück, and H. Müller-Steinhagen. *Materialuntersuchungen für chemische Langzeitwärmespeicher*, OTTI-20. in *Symposium Thermische Solarenergie. 2010*
- [20] Hauer, A. and F. Fischer, Open Adsorption System for an Energy Efficient Dishwasher. *Chemie Ingenieur Technik*, 2011. 83(1-2): p. 61-66.
- [21] Ugur, B., *Thermal Energy Storage in Adsorbent Beds*, 2013, Université d'Ottawa/University of Ottawa.

- [22] Dicaire, D. and F.H. Tezel, Regeneration and efficiency characterization of hybrid adsorbent for thermal energy storage of excess and solar heat. *Renewable Energy*, 2011. 36(3): p. 986-992.
- [23] Yu, N., R.Z. Wang, and L.W. Wang, Sorption thermal storage for solar energy. *Progress in Energy and Combustion Science*, 2013. 39(5): p. 489-514.
- [24] COMSOL, I., Burlington, MA, USA. COMSOL Multiphysics®. 2014. Version 5.0. Available from: <https://www.comsol.com/>.
- [25] Gleuckauf, E. and J. Coates, The influence of incomplete equilibrium on the front boundary of chromatograms and the effectiveness of separation. *J Chem Soc*, 1947. 1315: p. e21.
- [26] Chihara, K. and M. Suzuki, Air drying by pressure swing adsorption. *JOURNAL OF CHEMICAL ENGINEERING OF JAPAN*, 1983. 16(4): p. 293-299.
- [27] Geankoplis, C.J., Transport processes and separation process principles 2003: Prentice Hall Professional Technical Reference.
- [28] Hashi, M., J. Thibault, and F. Tezel, Recovery of ethanol from carbon dioxide stripped vapor mixture: adsorption prediction and modeling. *Industrial & Engineering Chemistry Research*, 2010. 49(18): p. 8733-8740.
- [29] Wang, Y. and M.D. LeVan, Adsorption equilibrium of carbon dioxide and water vapor on zeolites 5A and 13X and silica gel: pure components. *Journal of Chemical & Engineering Data*, 2009. 54(10): p. 2839-2844.
- [30] Geankoplis, C.J., Solutions Manual to Accompany Transport Processes and Separation Process Principles: (includes Unit Operations) 2003: Prentice Hall Professional Technical Reference.
- [31] Bergman, T.L. and F.P. Incropera, Introduction to heat transfer 2011: John Wiley & Sons.
- [32] Anderson, D.A., J.C. Tannehill, and R.H. Pletcher, Computational fluid mechanics and heat transfer. 1984.
- [33] Ergun, S., Fluid flow through packed columns. *Chem. Eng. Prog.*, 1952. 48: p. 89-94.